High efficient phosphate removal by lanthanum modified hydroxyapatite with a phase transformation process

Zhongjun Li[a,b], Qiwu Wei[a,b], Guisheng Zeng[a,b,*], Zhong Ren[a,b,*], Baojin Huang[a,b]

[a]*Key Laboratory of Jiangxi Province for Persistent Pollutants Control and Resources Recycle, Nanchang Hangkong University, Nanchang 330063, China, Tel. +86 13767957398; emails: gszeng@nchu.edu.cn (G. Zeng), renzhong424@163.com (Z. Ren), 432399946@qq.com (Z. Li), 913720070@qq.com (Q. Wei), huangjinbao76@126.com (B. Huang)*
[b]*National-Local Joint Engineering Research Center of Heavy Metals Pollutants Control and Resource Utilization, Nanchang Hangkong University, Nanchang 330063, China*

ABSTRACT

It is urgent to develop a cost-efficient phosphorus adsorbent for wastewater treatment. In this study, lanthanum modified hydroxyapatite (La-HAP) has been synthesized as an adsorbent for removing phosphorus in aqueous. The effects of physical and chemical parameters for adsorbent adsorption ability such as initial pH, contact time, initial phosphate concentration, and competing anions were investigated. Phosphate adsorption on La-HAP was fitted well by the Langmuir equation ($R^2 = 0.991$) and the maximum single-layer adsorption capacity is estimated to be 42.92 mg g^{-1} at 298 K. In addition, the kinetic studies showed that the phosphate adsorption data followed a pseudo-second-order model. The relatively high pH and competing anions have little influence on the adsorption performance. The La-HAP samples were characterized by Brunauer–Emmett–Teller, scanning electron microscopy-mapping, X-ray diffraction, and X-ray photoelectron spectroscopy methods. The analysis revealed that the solid phase transformation is the mechanism of phosphate removal.

Keywords: Lanthanum; Hydroxyapatite; Phosphate removal; Solid-phase transformation

1. Introduction

Eutrophication is one of the serious water pollutions in the world today. Large amounts of phosphorus effluent discharges of industrial wastewater and sewage direct emissions into lakes and rivers lead to eutrophication [1]. The eutrophication water makes algae grow abundantly consuming oxygen and resulting in the death of aquatic organisms and hence further aggravate water pollution [2]. The investigation shows that phosphorus is the main control factor of water eutrophication. If the content of phosphorus in water exceeds 0.02 mg L^{-1}, it will result in eutrophication [3]. Thus, phosphorus removal from wastewater is important to prevent eutrophication. Strict phosphorus wastewater discharge standards were set up in many countries [4], for example in American Environmental Protection Agency (EPA) regulations phosphorus concentration in wastewater discharged into lakes and reservoirs cannot be more than 0.05 mg L^{-1}.

In recent decades the methods of phosphorus removal in wastewater have been discussed and studied in order to meet the standards [5]. According to the method of phosphorus removal, chemical [6], and biological [7] methods are common, which including chemical precipitation [8], adsorption [9], electrodialysis, and so on. Adsorption is a highly efficient economic simple in process convenient in operation and easy to recycle attracted broad attention and studies [10]. The key of the adsorption method is to find an efficient adsorbent, adsorption material can be divided into natural materials such as modified bentonite [11],

* Corresponding authors.

hematite [12], zeolite [13,14], kaolin [15], waste-derived adsorbents such as steel slag [16], fly ash [17], and synthetic materials [16] such as magnetic iron oxide nanoparticles [18], activated carbon fiber [19], metal-organic frameworks materials [20], etc. It is can be found that among those materials, the adsorbent modification by lanthanum is a hot spot [9,17,19,21,22]. This can be ascribed to the high-affinity lanthanum to phosphorus. The essential of lanthanum-containing adsorbent is to find a suitable supporter for lanthanum. It must stable, easy to synthesis, cost-effective, size-controllable, and high environmental compatibility.

The hydroxyapatite is an outstanding material in environmental remediation, especially for heavy metal removal [23–25]. However, hydroxyapatite does not have the ability to binding phosphorus, but it may load lanthanum easy and stable. Therefore, after lanthanum loading, the modified hydroxyapatite may show great potential for phosphorus removal.

Therefore, the objectives of this study are to (1) synthesize lanthanum modified hydroxyapatite by ultrasonic-assisted chemical precipitation; (2) examine the phosphate adsorption performance of lanthanum modified hydroxyapatite, and optimize the condition; (3) characterize the synthesized lanthanum modified hydroxyapatite with X-ray diffraction (XRD), scanning electron microscopy (SEM), and X-ray photoelectron spectroscopy (XPS) to clarify the reaction mechanisms.

2. Experimental

2.1. Materials

Hydroxyapatite, lanthanum oxide, KH_2PO_4 (99%), hydrochloric acid, ammonia, sodium hydroxide, ascorbic acid, and molybdenum acid ammonium were purchased from Sinopharm Chemical Reagent Co., Ltd., (China). All the chemical reagents used were of analytical grade. The deionized (DI) water with a specific conductivity of 18 MΩ cm was used to prepare all solutions unless otherwise specified. A 1,000 mg P L^{-1} stock solution of phosphate was prepared by dissolving 4.434 g of KH_2PO_4 in 1,000 mL DI water. All phosphate in this study refers to orthophosphate unless otherwise specified.

2.2. Preparation of modified hydroxyapatite

Lanthanum modified hydroxyapatite was prepared by ultrasonic-assisted chemical precipitation. In brief, a 1 mol L^{-1} of HCl solution was added into 50 mg of Lanthanum oxide solution in 500 mL beakers for Lanthanum oxide completely dissolved. The hydroxyapatite (noted as HAP) was added to a 0.1 mol L^{-1} of lanthanum(III) solution at a ratio of 100:1 as solution:solid to form an aqueous suspension. The suspension was magnetically stirred for 30 min and follows an ultrasonic treatment for 30 min. The solid was separated by filtration and washed several times with deionized water to remove the superficially held impurities. The procedure of filtration and washing were repeated twice in order to obtain the La modified hydroxyapatite. The solid was dried for 8 h in an oven at 343 K and crushed in an agate mortar. Then the power set in the Porcelain

crucible at 773 K in the muffle furnace roasting 5 h finally placed materials in 343 K oven for use (noted as La-HAP).

2.3. Batch adsorption studies

Batch experiments consisted in analyzing the effect of initial aqueous concentration contact time solutions pH adsorbent dosage and temperature on phosphate adsorption onto La-HAP. These experiments were conducted at 303 ± 0.2 K in 150 mL conical flask. During these assays a predetermined amount of the adsorbent was shaken in 50 mL of phosphate solution during 24 h at 180 rpm using a magnetic stirrer. This time is high enough to ensure an equilibrium state between aqueous phosphate and the adsorbent. The dissolved phosphate concentration was determined spectrophotometrically after the suspension filtration through the filter disk with a pore size of 0.22 mm.

2.3.1. Impact of the adsorbent dosage

The impact of the adsorbent dosage on the phosphate adsorption onto La-HAP was determined for 100 mg L^{-1} initial aqueous concentration and at pH 7. The tested adsorbent doses varied from 3 to 7 g L^{-1}.

2.3.2. Phosphate adsorption isotherms (effect of initial phosphate concentrations)

Phosphate adsorption isotherms were conducted as follows: the sorbent (0.25 g) was added to a conical flask with a solution (50 mL) containing a certain amount of concentration of phosphate (10–500 mg P L^{-1}). The initial pH of phosphate solution was adjusted to 6.5–7.0 using 0.1 M HCl or 0.1 M NaOH. Then the flask was sealed and placed at a thermostatic shaker at 30°C for 24 h. The sample was filtered by using a 0.22 μm membrane filter and the phosphate concentrations in filtrates were analyzed by the ammonium molybdate spectrophotometric method [26]. The equilibrium adsorption amount of phosphate was calculated by the equation:

$$Q_e = \frac{V(C_0 - C_e)}{m} \tag{1}$$

where Q_e is the adsorption capacity (mg g^{-1}), C_0 is the initial concentration of phosphate (mg P L^{-1}), C_e is the equilibrium phosphate concentration, V is the volume of phosphate solution (L), and m is the sorbent mass (g). In order, Langmuir isotherm and Freundlich isotherm models [27] were used to explore their adsorption type.

The Langmuir equation and the Freundlich equation can be written in the following forms:

$$Q_e = Q_m \frac{K_l}{1 + K_l C_e} \tag{2}$$

$$Q_e = K_f C_e^{\frac{1}{n}} \tag{3}$$

where Q_e and C_e represent the adsorption capacity of adsorbents from experiment and the equilibrium phosphate

concentration (mg L^{-1}), respectively. K_1 is the Langmuir constant, and Q_m is the max adsorption capacity by the Langmuir calculation, K_f and n are the Freundlich constants, K_f indicates the sorption capacity and represents the strength of the absorptive bond, n is the heterogeneity factor which represents the bond distribution [28].

2.3.3. Phosphate adsorption kinetics

The adsorption kinetic study for P was performed by the dynamic adsorption experiment. For each operation, 0.25 g of the adsorbent was added into 50 mL of phosphate solution with an initial concentration of 100 mg P L^{-1}. The pH of the aqueous solution was adjusted to 6.5–7.0 with 0.1 M HCl or 0.1 M NaOH and then placed at a thermostatic shaker at 30°C. 1 mL of the solution was taken out of the polypropylene bottle at specified time intervals by syringe and filtered using a 0.22 μm membrane filter. The kinetic data were fitted with pseudo-first-order (Eq. (4)) and pseudo-second-order (Eq. (5)) [27]:

$$q_t = q_e \left(1 - e^{-k_1 t}\right) \tag{4}$$

$$q_t = \frac{q_e k_2 t}{1 + q_e k_2 t} \tag{5}$$

where k_1 (g mg^{-1} min^{-1}) and k_2 (g mg^{-1} min^{-1}) represent the first and second-order rate constant of adsorption; q_e (mg g^{-1}) the amount of phosphate adsorbed onto La-HAP at equilibrium time and q_t (mg g^{-1}) is the amount of phosphate adsorbed at time t (min).

2.3.4. Influence of coexisting anions on phosphate adsorption

The effect of common anions in wastewater on phosphate adsorption is related to its application prospect. Different anions: Cl$^-$, SO$_4^{2-}$, CO$_3^{2-}$, and F$^-$ were added into phosphate solutions. (100 mg P L^{-1} and 100 or 1,000 mg L^{-1} coexisting anions, for example, 100 mg Cl$^-$), 0.25 g of adsorbent was added to 50 mL, the mixed solutions. The initial pH of solution was adjusted to 6.5–7.0. After 24 h for equilibrium, the samples were filtered and the residual phosphate concentrations were measured.

2.3.5. Influence of pH on phosphate adsorption

To investigate the effect of pH on phosphate adsorption, 0.25 g of the adsorbent was added to 50 mL of a 100.0 mg P L^{-1} phosphate solution at different initial pH values ranging from 3.0 to 11.0 at 303 K. The initial pH of the phosphate solution was adjusted with 0.1 M NaOH and or HCl solutions.

The concentrations of sulfate, carbonate, chloride, and fluoride were analyzed on an ion chromatograph (883 Basic IC plus, Metrohm).

2.4. Material characterization

Surface morphology of La-HAP were observed with SEM using a JSM-6700 F instrument (JEOL Co., Ltd., Japan).

Fourier transform infrared (FT-IR) measurements were performed on a Nicolet FT-IR 380 instrument (Thermo Scientific Co., Ltd., USA). The specific surface area was determined from the adsorption branch of isotherm using the Brunauer–Emmett–Teller (BET) method in a relative pressure range of 0.05–0.30. The semiquantitative chemical composition and surface chemical states of the samples were examined by an X-ray photoelectron spectrometer (PHI 5600 Physical Electronics Inc., USA) with Al Ka radiation (1,486.6 eV).

3. Results and discussion

3.1. Characterization of adsorbent

X-ray powder diffraction patterns of the parent and modified La-HAP are shown in Fig. 1. For the raw HAP, the peaks located at 25.9°, 31.79°, 32.22°, 32.92°, and 39.82° are corresponding to diffractions from (002), (121), (112), (300), and (310) planes of HAP respectively, which coincided with the standard data of JCPDS Card No. 84-1998 for the hydroxyapatite Ca$_5$(PO$_4$)$_3$(OH). The narrow and strong diffractions indicate that the crystallinities of the HAP are good.

For the La-HAP, the weak and board diffractions indicate that the crystallinities of the La-HAP are low. After the search and match process by Jade 6.5, it is can be inferred that the La-HAP contains the phase of lanthanum hydrogen phosphate hydrate (PDF#34-0026 and PDF#34-0026) and a little hydroxyapatite. This result indicated that the Hydroxyapatite will be transformed to lanthanum hydrogen phosphate hydrate in the present of La^{3+}.

The SEM of HAP and La-HAP is shown in Fig. 2. By comparing Figs. 2a with b, distinct differences are founded. It is clear from Fig. 2a that the shape of HAP is an aggregated long sharp sliver with a length of about 200 nm. Consistent with previous research reports [29]. In Fig. 2b, it can be seen that the size of La-HAP was decreased slightly,
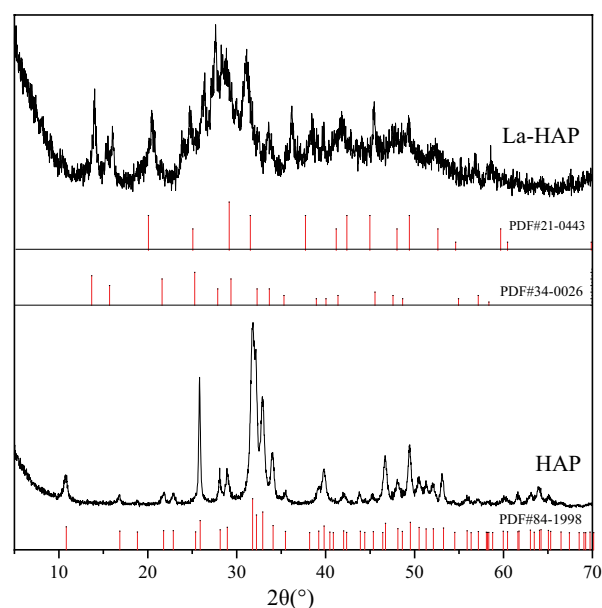

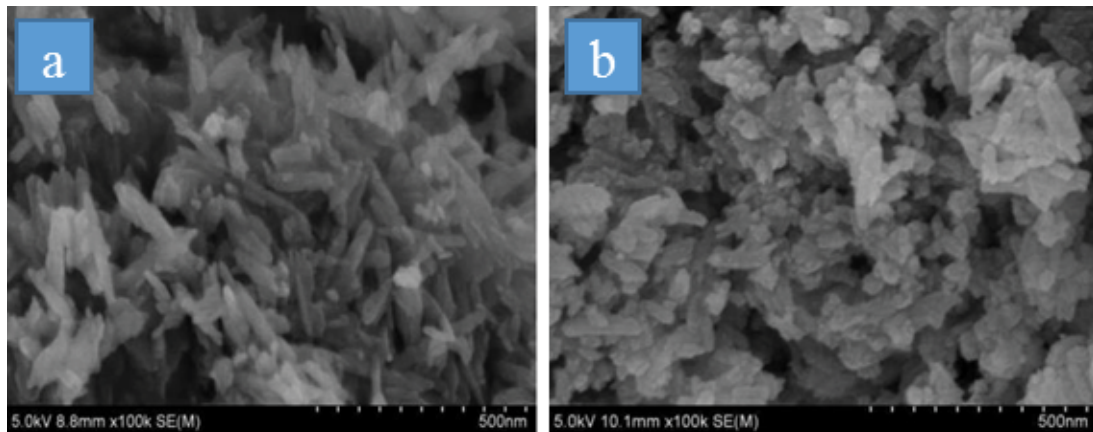Fig. 1. X-ray powder diffraction patterns of the HAP and La-HAP.

Fig. 2. SEM photographs of hydroxyapatite (a) and modified hydroxyapatite (b).

and the shape of La-HAP become obtuse. The surface roughness also increased. The morphology indicated that the La-HAP exhibits a lower crystalline which coincides with the XRD result. Concurrent elemental mapping confirms the formation of La-HAP nanocomposite as La, Ca, and O elements exist and uniform distribution throughout the material matrix (Fig. 3).

The BET specific surface area of HAP (a) and La-HAP (b) was 66.42 and 80.60 $m^2\ g^{-1}$, respectively. These areas are higher than those observed for Phoslock® (39.3 $m^2\ g^{-1}$) [11].
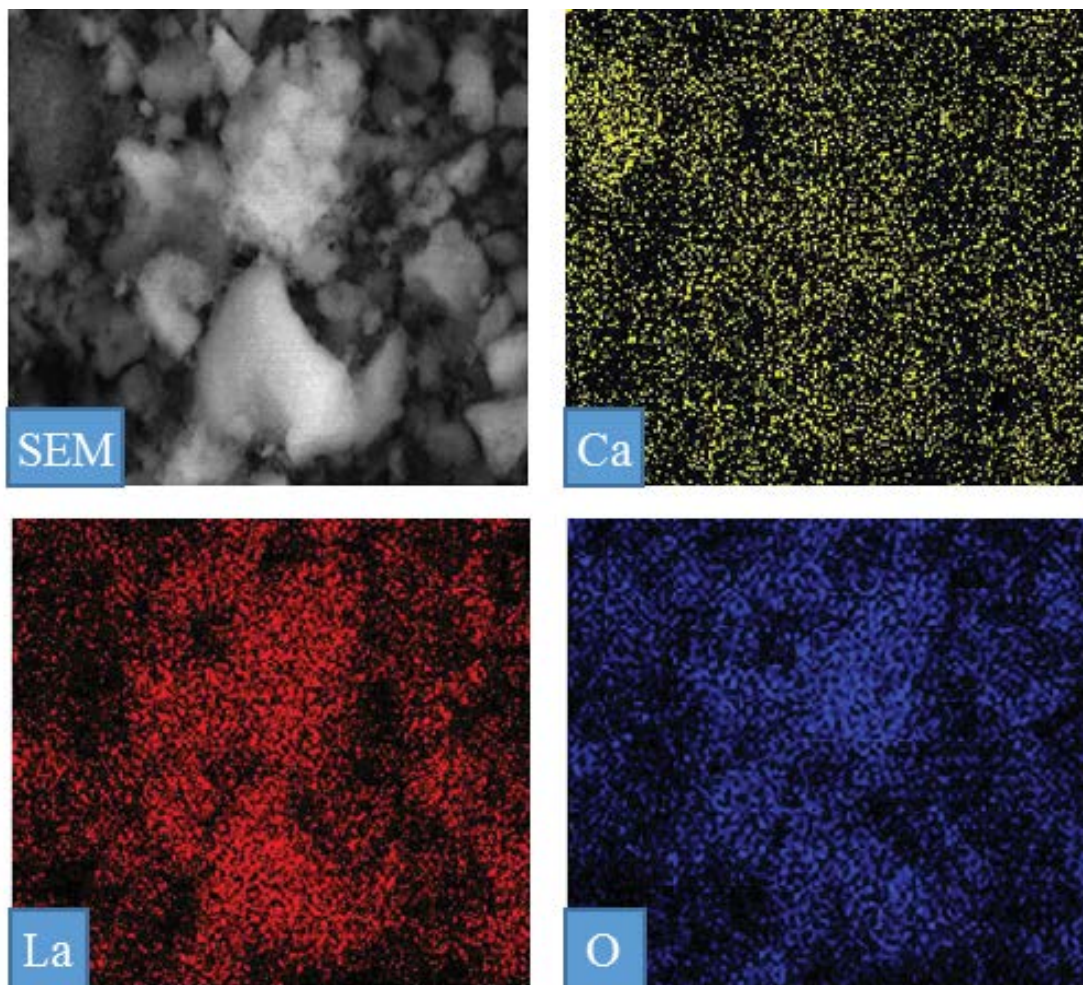

Fig. 3. Mapping of modified hydroxyapatite.

The significant increase of the specific surface area after lanthanide modification may ascribe to the formation of smaller and roughness nanocomposite. Nitrogen adsorption–desorption isotherms of the solids are illustrated in Fig. 4. The total pore volume of the HAP and La-HAP was 0.254 and 0.157 cm^3 g^{-1}, respectively. This indicated that the micropore in La-HAP is much more than HAP, for the higher specific surface area and lower total pore volume.

3.2. Adsorption studies

3.2.1. Effect of initial phosphate concentrations

According to the experimental conditions detailed in section 2.3 (Batch adsorption studies) the results (Fig. 5) show that phosphate adsorption efficiency and adsorption capacity show different trends. The phosphate adsorption amount increased with increasing initial phosphate concentration. In fact, raising the initial phosphate concentration from 10 to 500 mg L^{-1} makes the adsorption amount of La-HAP to increase from 1.96 to 43.52 mg g^{-1} respectively. This finding could be explained by the fact that the higher is the initial aqueous phosphate concentrations the higher is the concentration gradient between the aqueous solution and the solid phase, which result in high adsorption potential. On the contrary, the phosphate removal efficiency was decreased from 93% to 53%.

3.2.2. Effect of adsorbent dosage

The impact of the La-HAP dosage on phosphate removal from the aqueous solutions was investigated. The experimental results showed that the removal efficiency of phosphate increased slightly with increasing the amount of the adsorbent (Fig. 6). The extent of phosphate removal increases from 96.2% to 97.6% for the adsorbent doses of 3 to 7 g L^{-1}, respectively. Then the phosphate adsorption efficiency onto La-HAP remained quasi constant from an adsorbent dose of 5 g L^{-1} and further dose augmentation (until 5 g L^{-1}) did not affect significantly the uptake of phosphorus

from the aqueous solution. This plateau corresponds to an average residual phosphorus concentration at equilibrium (C_e) of 100 mg L^{-1} and removal efficiency of about 97.59%. Thus, under the studied experimental conditions, La-HAP present a relatively high phosphorus removal from aqueous solutions for doses equal or larger than 5 g L^{-1}.

3.2.3. Adsorption isotherms

The adsorption isotherm of the La-HAP was measured to assess its phosphate uptake capacity (Fig. 7) as a function of phosphate concentration. Langmuir and Freundlich models were employed to fit the isotherm data. To minimize the respective error functions a nonlinear fit was used to calculate the isotherm parameters. The fitted parameters of isotherm are provided in Table 1.

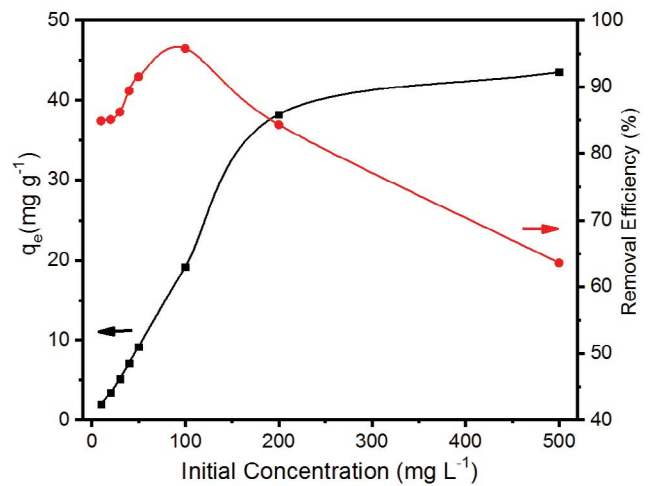It is shown that the phosphate adsorption of La-HAP can be better fitted to Langmuir model with relatively

Fig. 5. Influence of initial concentration of phosphate wastewater on adsorption capacity and adsorption efficiency.
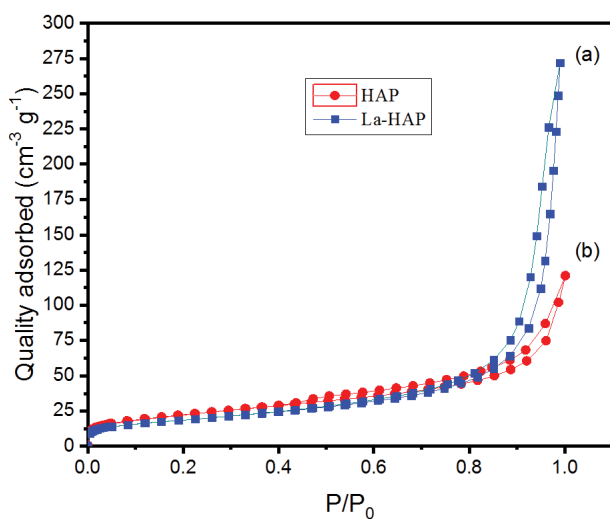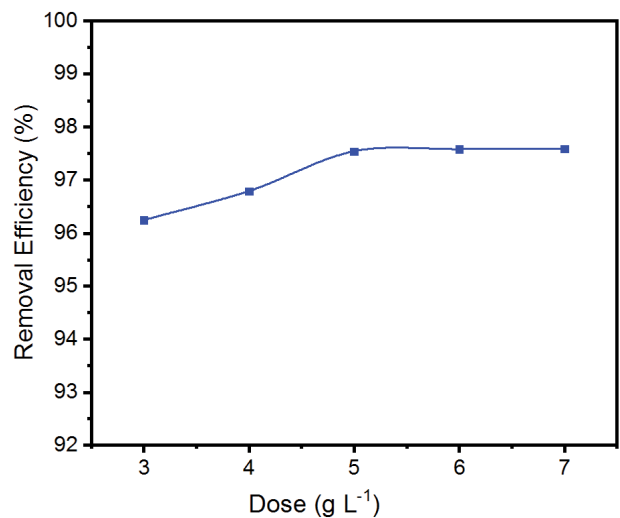
Fig. 4. BET of HAP and La-HAP.

Fig. 6. Effect of the dosage on the adsorption efficiency

higher R^2 values (R^2 = 0.9910) compared to Freundlich equation (R^2 = 0.7942) suggesting a monolayer phosphate adsorption onto the homogeneous sites of the La-HAP [30]. The adsorbent has a very high adsorption affinity to phosphate and the maximum phosphate adsorption capacity was estimated to be 42.92 mg P g^{-1} at 298 K by Langmuir model. Compared to other La-based adsorbents reported for phosphate (Table 2) La-HAP clearly exhibits superior capacity. For example, the maximum adsorption capacities of La-doped vesuvianite [31] and commercial Phoslock® [11] were only 27.8 and 10.5 mg P g^{-1},

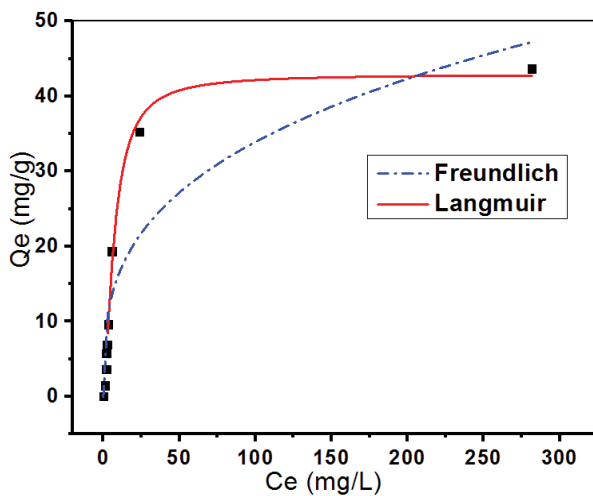respectively which were much lower than that of La-HAP in this work. The higher phosphate adsorption capacity of La-HAP to other La-modified adsorbents could be understood from the differences in the contents of active sites (i.e., La-O or –OH) that are responsible for phosphate uptake.

3.2.4. Adsorption kinetics

Adsorption kinetic studies were performed to evaluate the rate of phosphate uptake from solution with varying contact time. Fig. 8 shows the effect of contact time on the adsorption of phosphate by La-HAP. The phosphate uptake was very rapid in the first 5 min and adsorption equilibrium was almost achieved within 20 min. To further understand the phosphate adsorption process the kinetic data were fitted using pseudo-first-order and pseudo-second-order models (Eqs. (4) and (5)). The fitting parameter is shown in Table 3. The results show that both kinetic models can well describe the adsorption kinetic data with high correlation coefficient values (R^2 > 0.994). The higher R^2 values obtained with pseudo-second-order
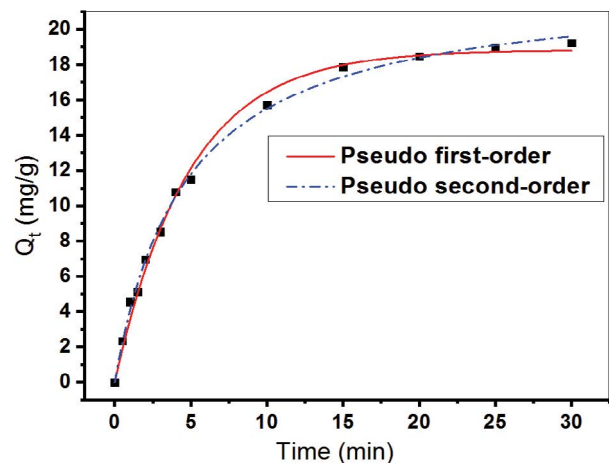

Fig. 7. Adsorption isotherm of La-HAP.

Fig. 8. Adsorption kinetics curve of lanthanum hydroxide modified hydroxyapatite.

Table 1
Fitted parameters for the pseudo-second-order kinetics and Langmuir isotherm of phosphate adsorption on La-HAP

Langmuir equation			Freundlich equation		
Q_m (mg g^{-1})	K_L	R^2	K_F	n	R^2
42.92	0.049	0.991	7.773	3.127	0.794

Table 2
Comparison of the adsorption capacities of different adsorbents for phosphate removal

Adsorbent	Q_{max} (mg g^{-1})	Reference
Lanthanum-modified hydroxyapatite	43.7	This work
La/Al-modified pillared clay	13.0	[32]
Granulated ferric hydroxide	23.3	[33]
La-doped vesuvianite	19.9	[31]
La$_2$O$_3$-zeolite	24.5	[34]
Commercial Phoslock®	10.5	[11]
ACF-LaFe	29.4	[26]
Activated aluminium oxide	13.8	[33]
Synthesized La(OH)$_3$	35.1	[35]
Al(III)-modified bentonite	12.7	[36]
Fe(III)-modified bentonite	14.0	[37]

Table 3
Fitting result of adsorption kinetics

Pseudo-first-order			Pseudo-second-order		
Q_e (mg g^{-1})	k_1	R^2	Q_e (mg g^{-1})	k_2	R^2
18.82	0.0095	0.994	22.59	0.0097	0.997

model indicated that the phosphate adsorption on La-HAP is likely a process of chemisorption. Similar results were observed for phosphate adsorption by other lanthanum-based adsorbent such as La(OH)$_3$-modified exfoliated vermiculites [38], magnetite/lanthanum hydroxide [39]. The sorption rate constant k_2 was determined to be 0.0097 g (mg min)$^{-1}$ which was significantly higher than those of other lanthanum-based sorbents (e.g., 0.0018 g (mg min)$^{-1}$).

3.2.5. Effects of solution pH

As a general rule, the pH of the solution has a significant effect on the surface characteristics of the adsorbent particles [40]. Fig. 9 shows that the pH value of the solution is weakly influenced the removal efficiency of phosphate by La-HAP. The maximum adsorption efficiency is obtained at pH 3, as high as 97.85%, the adsorption efficiency is decreased slowly with the increased pH. Such behavior has also been observed during phosphate adsorption onto other La-based adsorbent [17]. The decrease of efficiency may be ascribed to two reasons, on one hand, increased pH values makes the surface of La-HAP to carry more negative charges and consequently much harder to attract the negatively charged phosphate; on the other hand, the competition between hydroxyl ions and phosphate for adsorption sites. However, the affinity of La-HAP to phosphate is strong enough, the La-HAP also obtained a high removal extent as 96% at pH 11. It is indicating that lanthanum modified hydroxyapatite has a strong anti-pH-interference ability, previous studies lanthanum doped vesuvianite also exhibit this trend. An opposite
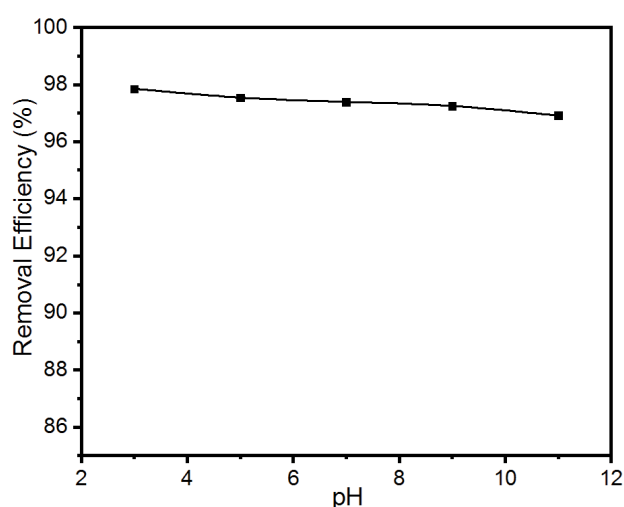
conclusion to magnetite/lanthanum hydroxide [39], the La-modified adsorbent drops to about 25% at pH 10.2, this may ascribe to a different form of lanthanum.

3.2.6. Effects of coexisting ions

In addition to rapid adsorption rate and high adsorption capacity, an ideal adsorbent should show a good selectivity. The potentially competing anions such as CO_3^{2-}, Cl$^-$, and SO_4^{2-} are mostly found in natural freshwater or wastewater, in addition, F$^-$ is the associated element of phosphorus. In order to evaluate the phosphate removal by La-HAP in practical water, the adsorption studies of phosphate in the presence of these coexisting ions were conducted and the results are presented in Fig. 10. It is clear that the coexisting anions can hardly affect the phosphate adsorption process on La-HAP, even at an initial concentration of 1,000 mg L^{-1}. The effects on adsorption of La-HAP follow the order: F$^-$ > CO_3^{2-} > SO_4^{2-} > Cl$^-$. Among the four anions, F$^-$ has strongest effect on the adsorption of phosphate on La-HAP. The presence of 100 mg L^{-1} to 1,000 mg L^{-1} F$^-$ can reduce the phosphate removal extent of La-HAP from 96.45% to 89.92%, respectively.

3.3. Adsorption mechanism

To reveal the adsorption mechanism, the chemical composition of the HAP before and after modified by La and the adsorbent after phosphate adsorption was measured by XPS. As shown in Fig. 11, the peaks are at the binding energy of 834.0, 529.0, 345, and 131 eV are attributed to La 3d, O 1s, Ca 2p, and P 2p. The elemental composition is shown in Table 4. The Ca element in raw HAP was of 19.43%, and almost disappeared in La-HAP and La-HAP after adsorption, indicated the transformation of hydroxyapatite to lanthanum hydrogen phosphate hydrate. The La element in La-HAP was of 14.44%, and decreased to 9.84%
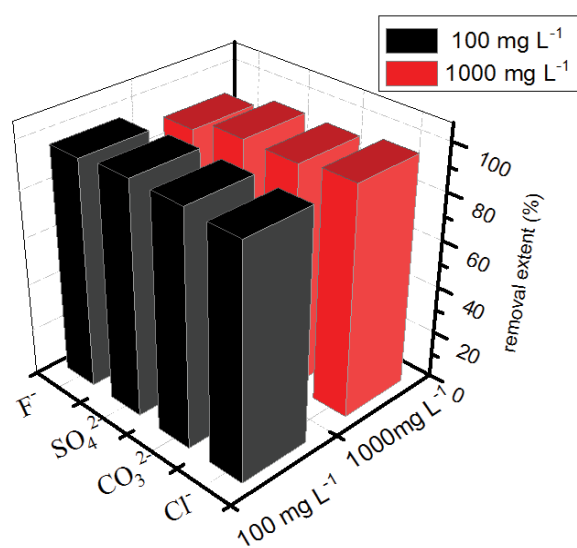

Fig. 9. Effect of pH on adsorption efficiency.

Fig. 10. Influence of co-existing ions on phosphate radical removal.

Table 4
XPS spectra of HAP, La-HAP, and La-HAP-P

	Element	Position	FWHM	Area	At%
	O 1s	529	2.436	44,421.68	66.96
HAP	Ca 2p	345	2.158	30,295.35	19.43
	P 2p	131	2.332	5,624.64	13.61
	O 1s	529	2.889	15,853.05	67.49
	Ca 2p	345	2.801	1,049.58	1.9
La-HAP	P 2p	131	3.207	2,365.75	16.17
	La 3d	833	6.441	39,665.61	14.44
	O 1s	529	2.659	27,336.03	70.44
La-HAP-P	Ca 2p	345	2.01	1,513.06	1.66
	P 2p	131	2.69	4,366.87	18.06
	La 3d	833	6.008	44,681.08	9.84

Fig. 11. XPS spectra of HAP, La-HAP, and La-HAP-P.

Fig. 12. X-ray powder diffraction patterns of the La-HAP and La-HAP-P.

superb adsorption capacity (42.92 mg P g⁻¹) at 298 K. The adsorption process effectiveness increased with increasing adsorbent dosage and decreased with increasing pH values. The maximum adsorption efficiency was attained at a 100 mg P L⁻¹ solution and it takes 30 min to reach the adsorption saturation. Phosphate adsorption equilibrium data were attended better with the use of the Langmuir model than the Freundlich model, indicating the phosphate removal was governed by monolayer adsorption. In addition, the adsorption kinetic data were better described by the pseudo-second-order model, which suggests the adsorption process was close to chemisorption. Uniform and dispersed adsorbent of lanthanum modified HAP and the phosphate is adsorbed to the adsorbent which can be observed at the results of SEM-mapping. The mechanism is identified by XPS and XRD. Our findings advance the use of La-based sorbents and highlight the described La-HAP nano-composite as a promising platform sorbent for high-selective phosphate removal from wastewater.

after phosphate adsorption. This may ascribe to the more phosphate were deposited in the solid phase, which coincides with the increased percentage of P 2p and O 1s.

The X-ray powder diffraction patterns of La-HAP after phosphate adsorption is shown in Fig. 12 (La-HAP-P), it is an obvious different to La-HAP. The La-HAP contain both PDF#21-0443 and PDF#34-0026, La-HAP-P mainly in PDF#21-0443 form. The molecular formula for PDF#34-0026 and PDF#21-0443 is $La_2(HPO_3)_3 \cdot 2H_2O$ and $LaHP_2O_7 \cdot 3H_2O$, respectively. It is can be concluded form the molecular formula, 1 mol La atom is bind 1.5 mol phosphate in PDF#34-0026, on the contrast, 1 mol La atom is bind 2 mol phosphate in PDF#21-0443. Therefore, the mechanism of phosphate removal is a phase transformation process.

4. Conclusion

This study provided an ultrasound-assisted precipitation method to prepare the lanthanum modified hydroxyapatite. In particular, the sample La-HAP exhibited a
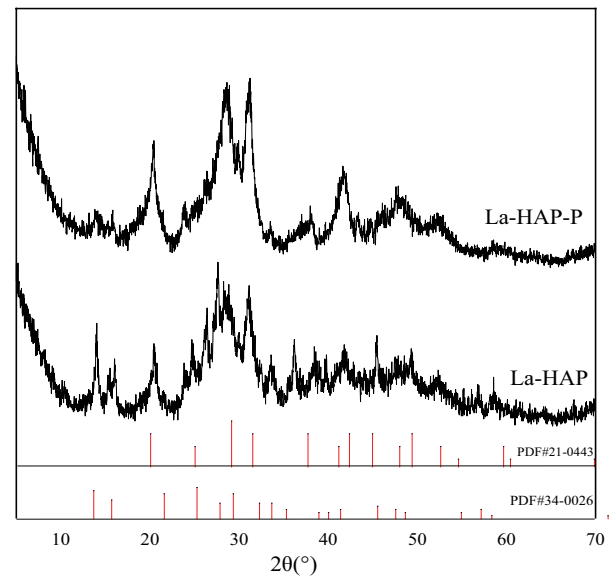
References

[1] Y. Jaffer, T.A. Clark, P. Pearce, S.A. Parsons, Potential phosphorus recovery by struvite formation, Water Res., 36 (2002) 1834–1842.

[2] J. He, W. Wang, F. Sun, W. Shi, D. Qi, K. Wang, R. Shi, F. Cui, C. Wang, X. Chen, Highly efficient phosphate scavenger based on well-dispersed La(OH)₃ nanorods in polyacrylonitrile nanofibers for nutrient-starvation antibacteria, ACS Nano, 9 (2015) 9292–9302.

[3] S. Jellali, M.A. Wahab, M. Anane, K. Riahi, L. Bousselmi, Phosphate mine wastes reuse for phosphorus removal from aqueous solutions under dynamic conditions, J. Hazard. Mater., 184 (2010) 226–233.

[4] T.H. Chen, J.Z. Wang, J. Wang, J.J. Xie, C.Z. Zhu, X.M. Zhan, Phosphorus removal from aqueous solutions containing low concentration of phosphate using pyrite calcinate sorbent, Int. J. Environ. Sci. Technol., 12 (2015) 885–892.

[5] M. Özacar, Adsorption of phosphate from aqueous solution onto alunite, Chemosphere, 51 (2003) 321–327.

[6] K. Suzuki, Y. Tanaka, K. Kuroda, D. Hanajima, Y. Fukumoto, T. Yasuda, M. Waki, Removal and recovery of phosphorous from swine wastewater by demonstration crystallization reactor and struvite accumulation device, Bioresour. Technol., 98 (2007) 1573–1578.

[7] D.P. Van Vuuren, A.F. Bouwman, A.H.W. Beusen, Phosphorus demand for the 1970–2100 period: a scenario analysis of resource depletion, Global Environ. Change, 20 (2010) 428–439.

[8] D. Kavak, Removal of boron from aqueous solutions by batch adsorption on calcined alunite using experimental design, J. Hazard. Mater., 163 (2009) 308–314.

[9] K. Reitzel, F.Ø. Andersen, S. Egemose, H.S. Jensen, Phosphate adsorption by lanthanum modified bentonite clay in fresh and brackish water, Water Res., 47 (2013) 2787–2796.

[10] C.M. Falkentoft, P. Harremoës, H. Mosbæk, The significance of zonation in a denitrifying, phosphorus removing biofilm, Water Res., 33 (1999) 3303–3310.

[11] F. Haghseresht, S. Wang, D.D. Do, A novel lanthanum-modified bentonite, Phoslock, for phosphate removal from wastewaters, Appl. Clay Sci., 46 (2009) 369–375.

[12] A.L. Gimsing, O.K. Borggaard, Phosphate and glyphosate adsorption by hematite and ferrihydrite and comparison with other variable-charge minerals, Clay Clay Miner., 55 (2007) 108–114.

[13] R. Chen, Q. Xue, Z. Zhang, N. Sugiura, Y. Yang, M. Li, N. Chen, Z. Ying, Z. Lei, Development of long-life-cycle tablet ceramic adsorbent for geosmin removal from water solution, Appl. Surf. Sci., 257 (2011) 2091–2096.

[14] D. Guaya, C. Valderrama, A. Farran, C. Armijos, J.L. Cortina, Simultaneous phosphate and ammonium removal from aqueous solution by a hydrated aluminum oxide modified natural zeolite, Chem. Eng. J., 271 (2015) 204–213.

[15] K.K. Al-Zboon, Phosphate removal by activated carbon–silica nanoparticles composite, kaolin, and olive cake, Environ. Dev. Sustainability, 20 (2018) 2707–2724.

[16] J. Xiong, Z. He, Q. Mahmood, D. Liu, X. Yang, E. Islam, Phosphate removal from solution using steel slag through magnetic separation, J. Hazard. Mater., 152 (2008) 211–215.

[17] J. Goscianska, M. Ptaszkowska-Koniarz, M. Frankowski, W. Franus, R. Panek, Removal of phosphate from water by lanthanum-modified zeolites obtained from fly ash, J. Colloid Interface Sci., 513 (2018) 72–81.

[18] A. Drenkova-Tuhtan, K. Mandel, A. Paulus, C. Meyer, F. Hutter, C. Gellermann, G. Sextl, M. Franzreb, H. Steinmetz, Phosphate recovery from wastewater using engineered superparamagnetic particles modified with layered double hydroxide ion exchangers, Water Res., 47 (2013) 5670–5677.

[19] L. Zhang, Q. Zhou, J. Liu, N. Chang, L. Wan, J. Chen, Phosphate adsorption on lanthanum hydroxide-doped activated carbon fiber, Chem. Eng. J., 185–186 (2012) 160–167.

[20] X. Min, X. Wu, P. Shao, Z. Ren, L. Ding, X. Luo, Ultra-high capacity of lanthanum-doped UiO-66 for phosphate capture: unusual doping of lanthanum by the reduction of coordination number, Chem. Eng. J., 358 (2019) 321–330.

[21] S. Ding, Q. Sun, X. Chen, Q. Liu, D. Wang, J. Lin, C. Zhang, D.C.W. Tsang, Synergistic adsorption of phosphorus by iron in lanthanum modified bentonite (Phoslock®): new insight into sediment phosphorus immobilization, Water Res., 134 (2018) 32–43.

[22] X. Yuan, G. Pan, H. Chen, B. Tian, Phosphorus fixation in lake sediments using LaCl₃-modified clays, Ecol. Eng., 35 (2009) 1599–1602.

[23] N. Jing, A. Zhou, Q. Xu, The synthesis of super-small nano hydroxyapatite and its high adsorptions to mixed heavy metallic ions, J. Hazard. Mater., 353 (2018) 89–98.

[24] J. Oliva, J. De Pablo, J. Cortina, J. Cama, C. Ayora, Removal of cadmium, copper, nickel, cobalt and mercury from water by Apatite II™: column experiments, J. Hazard. Mater., 194 (2011) 312–323.

[25] D. Wang, M. Paradelo, S.A. Bradford, W.J.G.M. Peijnenburg, L. Chu, D. Zhou, Facilitated transport of Cu with hydroxyapatite nanoparticles in saturated sand: effects of solution ionic strength and composition, Water Res., 45 (2011) 5905–5915.

[26] J. Liu, Q. Zhou, J. Chen, L. Zhang, N. Chang, Phosphate adsorption on hydroxyl-iron-lanthanum doped activated carbon fiber, Chem. Eng. J., 215–216 (2013) 859–867.

[27] J. Febrianto, A.N. Kosasih, J. Sunarso, Y. Ju, N. Indraswati, S. Ismadji, Equilibrium and kinetic studies in adsorption of heavy metals using biosorbent: a summary of recent studies, J. Hazard. Mater., 162 (2009) 616–645.

[28] I.H. Gubbuk, Isotherms and thermodynamics for the sorption of heavy metal ions onto functionalized sporopollenin, J. Hazard. Mater., 186 (2011) 416–422.

[29] D. Wang, S.A. Bradford, R.W. Harvey, B. Gao, L. Cang, D. Zhou, Humic acid facilitates the transport of ARS-labeled hydroxyapatite nanoparticles in iron oxyhydroxide-coated sand, Environ. Sci. Technol., 46 (2012) 2738–2745.

[30] Y. Li, C. Liu, Z. Luan, X. Peng, C. Zhu, Z. Chen, Z. Zhang, J. Fan, Z. Jia, Phosphate removal from aqueous solutions using raw and activated red mud and fly ash, J. Hazard. Mater., 137 (2006) 374–383.

[31] H. Li, J. Ru, W. Yin, X. Liu, J. Wang, W. Zhang, Removal of phosphate from polluted water by lanthanum doped vesuvianite, J. Hazard. Mater., 168 (2009) 326–330.

[32] S.L. Tian, P.X. Jiang, P. Ning, Y.H. Su, Enhanced adsorption removal of phosphate from water by mixed lanthanum/aluminum pillared montmorillonite, Chem. Eng. J., 151 (2009) 141–148.

[33] A. Genz, A. Kornmüller, M. Jekel, Advanced phosphorus removal from membrane filtrates by adsorption on activated aluminium oxide and granulated ferric hydroxide, Water Res., 38 (2004) 3523–3530.

[34] P. Ning, H.J. Bart, B. Li, X. Lu, Y. Zhang, Phosphate removal from wastewater by model-La(III) zeolite adsorbents, J. Environ. Sci., 20 (2008) 670–674.

[35] J. Xie, Z. Wang, S. Lu, D. Wu, Z. Zhang, H. Kong, Removal and recovery of phosphate from water by lanthanum hydroxide materials, Chem. Eng. J., 254 (2014) 163–170.

[36] L. Yan, Y. Xu, H. Yu, X. Xin, Q. Wei, B. Du, Adsorption of phosphate from aqueous solution by hydroxy-aluminum, hydroxy-iron and hydroxy-iron-aluminum pillared bentonites, J. Hazard. Mater., 179 (2010) 244–250.

[37] V. Kuroki, G.E. Bosco, P.S. Fadini, A.A. Mozeto, A.R. Cestari, W.A. Carvalho, Use of a La(III)-modified bentonite for effective phosphate removal from aqueous media, J. Hazard. Mater., 274 (2014) 124–131.

[38] W. Huang, D. Li, Z. Liu, Q. Tao, Y. Zhu, J. Yang, Y. Zhang, Kinetics, isotherm, thermodynamic, and adsorption mechanism studies of La(OH)₃-modified exfoliated vermiculites as highly efficient phosphate adsorbents, Chem. Eng. J., 236 (2014) 191–201.

[39] L. Fang, R. Liu, J. Li, C. Xu, L. Huang, D. Wang, Magnetite/lanthanum hydroxide for phosphate sequestration and recovery from lake and the attenuation effects of sediment particles, Water Res., 130 (2018) 243–254.

[40] N. Bektaş, H. Akbulut, H. Inan, A. Dimoglu, Removal of phosphate from aqueous solutions by electro-coagulation, J. Hazard. Mater., 106 (2004) 101–105.